

CLF-RL: Control Lyapunov Function Guided Reinforcement Learning

Kejun Li*, Zachary Olkin*, Yisong Yue, Aaron D. Ames

Abstract—Reinforcement learning (RL) has shown promise in generating robust locomotion policies for bipedal robots, but often suffers from tedious reward design and sensitivity to poorly shaped objectives. In this work, we propose a structured reward shaping framework that leverages model-based trajectory generation and control Lyapunov functions (CLFs) to guide policy learning. We explore two model-based planners for generating reference trajectories: a reduced-order linear inverted pendulum (LIP) model for velocity-conditioned motion planning, and a precomputed gait library based on hybrid zero dynamics (HZD) using full-order dynamics. These planners define desired end-effector and joint trajectories, which are used to construct CLF-based rewards that penalize tracking error and encourage rapid convergence. This formulation provides meaningful intermediate rewards, and is straightforward to implement once a reference is available. Both the reference trajectories and CLF shaping are used only during training, resulting in a lightweight policy at deployment. We validate our method both in simulation and through extensive real-world experiments on a Unitree G1 robot. CLF-RL demonstrates significantly improved robustness relative to the baseline RL policy and better performance than a classic tracking reward RL formulation.

I. INTRODUCTION

Achieving stable and agile bipedal locomotion remains a central challenge in robotics due to the high-dimensional, underactuated, and hybrid nature of legged dynamics, which combine continuous motion and discrete events such as foot-ground impacts. This hybrid behavior poses significant challenges for designing controllers that combine precise coordination with robustness for real-world deployment.

Traditional model-based control frameworks address these challenges through principled formulations such as trajectory optimization. Methods based on hybrid zero dynamics (HZD) [1] and feedback-linearization have enabled offline generation of stable walking gaits under physical and task constraints [2]. These techniques provide strong guarantees on stability and constraint satisfaction but require solving large-scale nonlinear programs that are computationally demanding and sensitive to model mismatch, limiting their practicality for deployment. To enable faster and more reactive planning, many approaches leverage reduced order models such as the linear inverted pendulum (LIP) and its variants [3], [4], which simplify the dynamics by focusing on the center of mass and foot placement. While computationally efficient and suitable for stabilization and mid-level planning, these models rely on strong assumptions such as massless legs and constant center of mass height, which limit

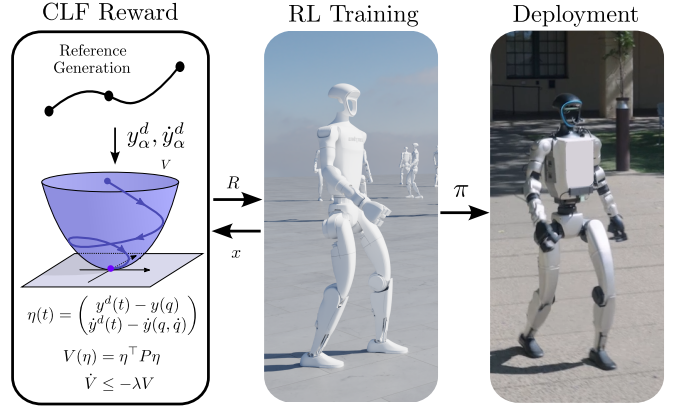


Fig. 1: Overview of our approach. A reference generator produces target trajectories, which are used to construct a CLF-based reward. An RL policy is trained in simulation with this reward and deployed on a real humanoid robot.

their ability to generate highly dynamic and agile whole body motion.

Recent advances in computation and GPU-parallelizable physics simulators have made reinforcement learning (RL) a promising alternative for locomotion control. By offloading the heavy computation to offline training in massively parallel simulations, RL enables lightweight policy inference during online deployment to hardware [5], [6], [7], [8], [9]. However, applying RL to bipedal locomotion remains challenging due to its reliance on heuristic reward design, which is tedious to construct, sensitive to tuning, and, if poorly shaped, can lead to unstable gaits, prolonged training, and poor sim-to-real transfer. A strategy to alleviate the burden of this process is to embed model-based reference trajectories directly into the RL reward. This idea has been explored using both reduced order models [10], [11] and full-order models within the HZD framework [12]. [13] proposes a different way to incorporate a LIP controller into RL by generating desired footstep locations during training and using it to provide feedback control for rough terrain.

While prior model-guided approaches improve structure during training, they typically reward only the instantaneous tracking error, treating two states with the same error magnitude equally—even if one is actively converging toward the reference and the other is diverging. This can cause policies to undervalue transient corrections. To address these limitations, we propose a reward shaping framework built on control Lyapunov functions (CLFs), a fundamental tool in nonlinear control theory for generating certifiably stable controllers [14], [15], [16]. CLFs have previously been used

* denotes equal contribution. This research is supported by Technology Innovation Institute (TII) and the National Science Foundation Graduate Research Fellowship.

in bipedal locomotion, often in conjunction with HZD, to formally guarantee the stability of periodic gaits [17] and have also been integrated into learning-based methods in other domains [18], [19]. For instance, [20] introduces a reward-reshaping method that incorporates a candidate CLF for fine-tuning policies using minimal hardware data.

Our approach embeds both the CLF and its associated decrease condition directly into the RL reward, where the decrease condition encodes a desired minimal convergence rate, providing meaningful intermediate rewards whenever the error is being reduced, similar to potential-based reward shaping, which has been shown to be more robust to scaling and hence simplify tuning [21]. This yields a reward component that is principled, easy to integrate, and less sensitive to manual reward balancing than conventional tracking formulations.

Building on these properties, we propose a structured reward shaping approach that combines model-based reference planning with CLF-inspired objectives to guide policy learning toward stable and robust behaviors (Fig. 1). We use two complementary planners for generating velocity-conditioned reference trajectories: (1) a reduced-order linear inverted pendulum (LIP) model for online generation, and (2) a precomputed hybrid zero dynamics (HZD) gait library from full-body offline trajectory optimization. Both produce periodic orbits but differ in fidelity and real-time suitability. From these trajectories, we construct a CLF $V = \eta^\top P \eta$, where η denotes the output tracking error. Once a reference trajectory is available, implementing the CLF decrease condition requires minimal effort: the tuning process is straightforward, involving far fewer reward terms than conventional rewards and resembling gain tuning in a tracking controller. The CLF and its associated stability condition is embedded into the RL reward to shape the policy to promote stable behaviors during training. We validate our approach through both simulation and hardware experiments on the Unitree G1 humanoid robot. Results demonstrate that CLF-based reward shaping improves tracking performance at high velocities, reduces variance under randomized model perturbations, and enhances robustness compared to standard RL baselines—offering a promising path toward more robust and theoretically grounded locomotion learning.

II. PRELIMINARIES

Consider a robotic system with generalized coordinates $q = [q_b^\top, q_a^\top]^\top \in \mathcal{Q} \subset \mathbb{R}^n$, where $q_b \in SE(3)$ denotes the floating-base coordinates and $q_a \in \mathbb{R}^m$ the actuated degrees of freedom (DoFs). The control input is $u \in \mathbb{R}^m$, and the full-order state is given by $x = [q^\top, \dot{q}^\top]^\top$.

A. Hybrid Dynamics

Legged locomotion is often modeled as a hybrid system with continuous dynamics and discrete transitions such as impact events across domains [1]. Let \mathcal{D} denote the domain and \mathcal{S} the guard of the system. The hybrid system \mathcal{H} can be

described as:

$$\mathcal{H} : \begin{cases} \dot{x} = f(x) + g(x)u & x \in \mathcal{D} \setminus \mathcal{S}, \\ x^+ = \Delta(x^-) & x^- \in \mathcal{S}, \end{cases} \quad (1)$$

$$(2)$$

where (1) represents the continuous full-order Lagrangian dynamics, while $\Delta : \mathcal{S} \rightarrow \mathcal{D}$ represents the discrete event when contact mode changes, and the superscripts “−” and “+” indicates the moments immediately before and after the discrete impact event, respectively.

Within each domain, the system dynamics can be derived from the Euler-Lagrange equation:

$$D(q)\ddot{q} + H(q, \dot{q}) = Bu + J_h(q)^T F \quad (3)$$

$$J_h(q)\ddot{q} + \dot{J}_h(q, \dot{q})\dot{q} = 0 \quad (4)$$

where $D(q) : \mathcal{Q} \rightarrow \mathbb{R}^{n \times n}$ is the mass-inertia matrix, $H : \mathcal{Q} \times T\mathcal{Q} \rightarrow \mathbb{R}^n$ contains the Coriolis and gravity terms, and $B \in \mathbb{R}^{n \times m}$ is the actuation matrix. The Jacobian of the holonomic contact constraint is $J_h(q) \in \mathbb{R}^{h \times n}$ and the associated constraint wrench is $F \in \mathbb{R}^h$.

B. Periodic Gait Generation

Legged locomotion is inherently periodic, alternating between stance and swing phases. This motivates analysis via step-to-step (S2S) dynamics, expressed by the discrete-time Poincaré return map $P : \mathcal{S} \rightarrow \mathcal{S}$, where $x_{k+1} = P(x_k)$ evaluates the state at successive impacts. A periodic gait corresponds to a fixed point x^* such that $P(x^*) = x^*$ and is exponentially stable if this fixed point is locally attracting [22].

Periodic gaits can be generated by shaping the return map to admit a stable fixed point. Here, we focus on two complementary approaches: full-order hybrid zero dynamics (HZD) and H-LIP models.

Hybrid Zero Dynamics: The Hybrid Zero Dynamics (HZD) framework is a model-based approach for designing stable walking gaits for bipedal robots. It operates by enforcing a set of virtual constraints, typically specified using Bézier polynomials with coefficients α . These constraints define desired trajectories for joint or end-effector motion as functions of a monotonically increasing phase variable. Driving the output of the virtual constraints to zero renders the zero dynamics manifold, denoted \mathcal{Z}^α , invariant and attractive.

To achieve periodic walking under hybrid dynamics, the manifold must also be impact invariant, meaning that the system returns to \mathcal{Z}^α after a discrete event (e.g., foot impact):

$$\Delta(\mathcal{Z}^\alpha \cap \mathcal{S}) \subset \mathcal{Z}^\alpha \quad (5)$$

where Δ denotes the reset map and \mathcal{S} is the switching surface. When this condition holds, the system implicitly stabilizes a fixed point in the step-to-step dynamics.

Hybrid Linear Inverted Pendulum: Assuming constant angular momentum and a fixed p_{com}^z leads to the well-known Linear Inverted Pendulum (LIP) model, widely used in humanoid walking control [3], [23].

To account for the hybrid nature of bipedal walking, [24] proposed the Hybrid Linear Inverted Pendulum (H-LIP) model. Like the LIP, it assumes constant CoM height

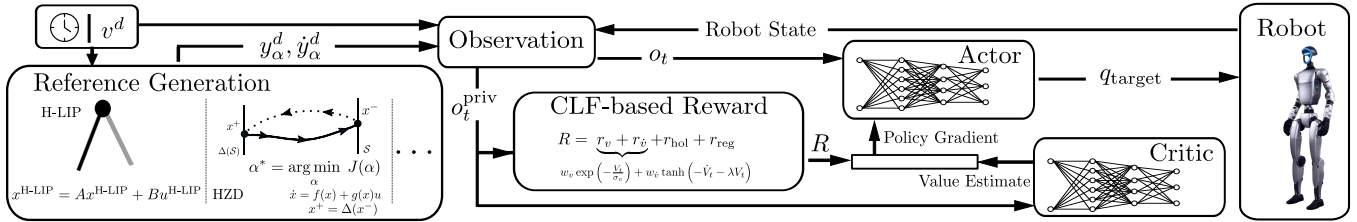


Fig. 2: Overview of the proposed CLF-guided reinforcement learning framework. A desired velocity v^d is passed to a reference generator (e.g., H-LIP or HZD) to produce targets $y_\alpha^d, \dot{y}_\alpha^d$. These, along with the robot state and privileged variables o_t^{priv} , are used to compute a CLF-based reward. The actor-critic policy is trained with this reward and outputs joint targets q_{target} for the robot.

and stepping frequency, but it explicitly models the hybrid walking dynamics of underactuated bipeds. The deviation between the full-order model and H-LIP is treated as a bounded error, enabling the design of state-feedback stepping controllers that stabilize horizontal CoM states within bounded invariant sets. The H-LIP dynamics for the single support phase (SSP) and double support phase (DSP) are given by:

$$a_{\text{com}}^{\{x,y\}} = \frac{g}{p_{\text{com}}^z} p_{\text{com}}^{\{x,y\}} \quad (\text{SSP}) \quad a_{\text{com}} = 0 \quad (\text{DSP})$$

where the p_{com}^z and domain duration ($T_{\text{SSP}}, T_{\text{DSP}}$) are constant. Assuming no velocity jump, we can combine the two domains with step size $u^{\text{H-LIP}}$ equivalently as:

$$\Delta_{\text{SSP}^- \rightarrow \text{SSP}^+} : \begin{cases} v_{\text{com}}^+ = v_{\text{com}}^- \\ p_{\text{com}}^+ = p_{\text{com}}^- + v_{\text{com}}^- T_{\text{DSP}} - u^{\text{H-LIP}}. \end{cases}$$

H-LIP model S2S dynamics are given by $x_{k+1}^{\text{H-LIP}} = Ax_k^{\text{H-LIP}} + Bu_k^{\text{H-LIP}}$, with $x^{\text{H-LIP}} = [p_{\text{com}}, v_{\text{com}}]^T$, which can be used to approximate the Poincaré return map of the full order system. For more details on the H-LIP model formulation and derivation of its step-to-step dynamics, we refer the reader to [24].

Remarks: While H-LIP enables fast online gait generation with foot placement feedback, our method uses only nominal planned trajectories, obtained by identifying the fixed point and computing the continuous trajectory analytically. Although HZD operates on full order dynamics and H-LIP relies on reduced order approximations, both regulate the return map to achieve stable periodic gaits, a shared focus that motivates our reward shaping framework.

C. Control Lyapunov Functions (CLFs)

For a nonlinear control-affine system of the form $\dot{x} = f(x) + g(x)u$, a continuously differentiable, positive definite function $V(x) : \mathbb{R}^{2n} \rightarrow \mathbb{R}$ is called an exponentially stabilizing control Lyapunov function (CLF) if there exists a control input u such that

$$\inf_u \nabla_x V(x)(f(x) + g(x)u) < -\lambda V(x). \quad (6)$$

for scalar $\lambda > 0$. This inequality guarantees that $V(x)$ decreases along system trajectories, implying exponential

convergence of the state x to the origin (or a desired manifold).

For hybrid systems such as bipedal locomotion with discrete impact events, CLFs can still be applied within each continuous domain of the dynamics. Prior work has shown that if the rate of convergence in the continuous phase is sufficiently fast, it can offset the destabilizing effects of impacts [17], providing a principled way to certify stability despite hybrid transitions.

Importantly, the CLF condition (6) defines a set of admissible control inputs rather than a unique control law. Any control input u that satisfy the inequality contributes to stability. This property makes CLFs especially appealing for reinforcement learning: rather than enforcing a fixed feedback controller, we can embed the CLF condition directly into the reward function, encouraging the policy to learn Lyapunov-stable behavior, without constraining it to a specific control structure.

III. REFERENCE-GUIDED REWARD SHAPING

We consider the reinforcement learning (RL) problem of learning a locomotion policy $\pi_\theta(a_t|o_t)$ that maps proprioceptive observations o_t to actions a_t . The policy is trained using Proximal Policy Optimization (PPO) [25], a widely used actor-critic method that optimizes a clipped surrogate objective with entropy regularization. Instead of relying solely on sparse or handcrafted rewards, we embed model-based prior knowledge into the reward through a control Lyapunov function (CLF), promoting stability with respect to a reference trajectory. The overall framework, including reference generation and CLF-based reward shaping, is illustrated in Fig. 2.

A. Reference Trajectory Generation

Our approach assumes access to a nominal reference trajectory that encodes a periodic or quasi-periodic walking motion given a desired velocity. In this work, we focus on two sources of reference trajectories: the H-LIP model and full-order HZD optimization. However, the framework is agnostic to the origin of the trajectory.

H-LIP-Based Reference: Given a target walking velocity v^d , we first solve for the H-LIP fixed point $x^* = Ax^* + Bu^*$, where the step size $u^* = v^d T$ corresponds to the

desired walking speed and nominal step time. This yields a periodic center-of-mass (CoM) state $x^* = [p_{\text{com}}, v_{\text{com}}]^\top$ consistent with the H-LIP step-to-step dynamics. Using this fixed point, we analytically generate the CoM trajectory over one step. The swing foot trajectory is constructed using a time-parameterized 5th-order Bézier curve to ensure foot clearance and smooth touchdown. For other end-effector or joint trajectories (e.g., torso pitch, knees, or arms), we use simple sinusoidal patterns that are synchronized with the gait phase. This procedure produces time-varying desired trajectories for the end effectors and joints.

HZD-Based Reference: To obtain HZD trajectories, we solve an offline trajectory optimization problem to determine the Bézier coefficients α that define the virtual constraints:

$$\alpha^* = \arg \min_{\alpha} J(\alpha)$$

s.t. Closed-loop dynamics,

Hybrid invariance (Eq. (5)),

Physical constraints (e.g., torque, joint limits),

$$y(q(t)) = B(\tau(t); \alpha).$$

Here, $y(q)$ denotes the controlled outputs, and $B(\tau; \alpha)$ is the Bézier-parameterized desired trajectory. The phase variable $\tau(t) = \phi(q, t)$ indicate the progression along the trajectory. In our implementation, τ is time-based, however, a common alternative is a state-based phase variable, such as the horizontal hip displacement, which ensures monotonicity. This setup guarantees that the Bézier curve is evaluated at the correct phase value during optimization.

The optimized trajectory specifies desired joint or end-effector positions and velocities as functions of phase over a single step with one stance leg. Once a single step is solved, the solution is symmetrically remapped to produce a full gait cycle with alternating stance legs, yielding reference trajectories for the complete walking motion.

B. CLF-Based Reward Terms

We denote the output error between the current state and reference trajectory as

$$\eta(t) = \begin{pmatrix} y^d(t) - y(q) \\ \dot{y}^d(t) - \dot{y}(q, \dot{q}) \end{pmatrix}$$

Based on this tracking error, we construct a control Lyapunov function as:

$$V(\eta) = \eta^\top P \eta,$$

This formulation implicitly assumes a double integrator reference model for the output dynamics, allowing us to define a Lyapunov function without explicitly computing Lie derivatives $L_f V$ or $L_g V$ for the full-order system. The matrix $P \succ 0$ is the unique solution to the Continuous-Time Algebraic Riccati Equation (CARE) corresponding to this linearized model.

To avoid explicitly computing $\dot{\eta}$ and \dot{V} , we approximate the Lyapunov derivative using finite differences:

$$\dot{V}_t \approx \frac{V_{t+1} - V_t}{\Delta t}, \quad \text{with } V_t = V(\eta(t)).$$

We define a CLF tracking reward:

$$r_v = w_v \exp\left(-\frac{V_t}{\sigma_v}\right) \quad (\text{CLF Tracking})$$

where $\sigma_v = \mu_{\text{max}}(P) \eta_{\text{max}}^2$, with $\mu_{\text{max}}(P)$ denoting the maximum eigenvalue of the CLF matrix P , η_{max} representing an empirical bound on the tracking error.

We consider two versions of the CLF decay condition: a smooth formulation using the hyperbolic tangent, and a clipped version:

$$r_v^{\text{tanh}} = w_v \tanh\left(-\left(\dot{V}_t + \lambda V_t\right)\right) \quad (\text{CLF Decay: Tanh})$$

$$r_v^{\text{clip}} = w_v \cdot \max\left(\min\left(\frac{\dot{V}_t + \lambda V_t}{\sigma_v}, 1\right), 0\right), \quad (\text{CLF Decay: Clipped})$$

where $\sigma_v = 2\|P\|\eta_{\text{max}}\dot{\eta}_{\text{max}} + \lambda\mu_{\text{max}}\eta_{\text{max}}^2$ and $\lambda > 0$ specifying the desired CLF decay rate. The tanh-based reward provides smooth gradients and naturally saturates large violations, but can overly dominate the overall reward depending on the relative weight between r_v and r_v . In contrast, the clipped version is less sensitive to weighting but requires careful normalization to ensure meaningful reward shaping, especially under significant domain randomization.

C. Other Reward Terms

In addition to the CLF terms, we incorporate several auxiliary rewards commonly used in RL for legged system:

Stance Foot Holonomic Reward: To enforce stance-foot holonomic constraints, we define a combined reward:

$$r_{\text{hol}} = w_{\text{hpos}} \exp\left(-\frac{\|p_{\text{st}} - p_{\text{st}}^0\|}{\sigma_p}\right) + w_{\text{hvel}} \exp\left(-\frac{\|v_{\text{st}}\|}{\sigma_v}\right),$$

where p_{st} and p_{st}^0 are the current and the initial stance foot positions when it enter the domain, v_{st} is the stance foot velocity, and $w_{\text{hpos}}, w_{\text{hvel}}$ are weighting terms.

Regularization Term: To discourage excessive control effort, abrupt actions, and joint limit violations, we include a regularization reward:

$$r_{\text{reg}} = -w_u \|u_t\|^2 - w_{\Delta a} \|a_t - a_{t-1}\|^2 - w_{q_{\text{limit}}} \|\max(0, q_{\text{min}} - q_t) + \max(0, q_t - q_{\text{max}})\|_1,$$

where each term is weighted by its corresponding coefficient to balance control effort, motion smoothness, and adherence to joint limits.

D. Total Reward

The final reward used for policy training is the weighted sum of all components:

$$R = r_v + r_v + r_{\text{hol}} + r_{\text{reg}},$$

This reward structure encodes both task performance and physical feasibility, allowing the policy to balance tracking, stability, and regularization objectives. By combining model-based references (e.g., from reduced-order planning or offline trajectory optimization) with CLF-inspired reward shaping and constraint-aware regularization, our framework embeds

control-theoretic structure into the reinforcement learning process. This guides training toward stable, robust, and physically plausible locomotion, while preserving the flexibility and adaptability of model-free RL.

IV. CLF-RL IMPLEMENTATION

We demonstrate our framework on the 29-DoF Unitree G1 humanoid robot, using 21 actuated degrees of freedom for motion planning. The hand and wrist joints are fixed during training and controlled with zero desired position and velocity during deployment.

Reference Generation: We use the same set of end-effector and joint positions for both HZD- and H-LIP-based trajectories. The full reference output $y_\alpha^d(t) \in \mathbb{R}^{n_y}$, with $n_y = 21$ is structured as follows:

$$y_\alpha^d = (p_{\text{com}}^d \quad \phi_{\text{pelvis}}^d \quad p_{\text{sw}}^d \quad \theta_{\text{sw}}^d \quad q_{\text{shoulder}}^d \quad q_{\text{elbow}}^d)^\top,$$

where the terms represent the desired CoM position, pelvis orientation, swing foot position and orientation, and arm joint angles. To account for turning motions during training, we heuristically adjust the reference trajectory based on the commanded angular velocity. Specifically, we modify the yaw orientation of all end-effector frames to align with the integrated yaw derived from the commanded angular velocity over time.

The HZD optimization is computed offline using IPOPT [26] and Casadi [27]. Hard constraints are used to enforce dynamics, periodicity, virtual constraints, and step length among others. The optimization problem is formulated as a multiple-shooting problem over a single swing phase.

Policy Structure: The policy receives a combination of proprioceptive and task-relevant inputs, including angular velocity, projected gravity, commanded linear and angular velocities, relative joint positions and velocities, the previous action, and a phase-based time encoding using $\sin(2\pi t/t_{\text{period}})$ and $\cos(2\pi t/t_{\text{period}})$. The stepping period t_{period} is set to 0.8 s, corresponding to a full gait cycle (i.e., two steps). The policy outputs joint position commands relative to a default symmetric standing pose at 50 Hz. This default pose is fixed across all policies we trained.

Both the actor and critic networks use a fully connected feedforward architecture with hidden layer dimensions of [512, 256, 128], using the ELU (Exponential Linear Unit) activation function at each layer. To facilitate learning, the critic (value network) receives additional privileged information o_t^{priv} not accessible to the actor, such as stance and swing foot linear and angular velocities, reference trajectory positions and velocities, and binary contact state indicators. These inputs help stabilize value estimation and improve training efficiency.

Training Procedure: We use *IsaacLab*, a GPU-accelerated simulation framework built on top of NVIDIA Isaac Sim, with its development initiated from the *Orbit* framework [28]. For policy training, we use the PPO implementation from Robotics System Lab RL library [29].

All training use the same set of terrain settings, robot models, and domain randomization parameters. To improve

policy robustness and facilitate transfer to hardware, we apply domain randomization to physical properties such as link masses, static and dynamic friction coefficients, and the center of mass position. Additionally, external perturbations are introduced by applying randomized velocity impulses in the x and y directions to the base link at fixed time intervals.

Training is conducted over a range of commanded velocities, with linear velocity $v_x \in [-0.75, 0.75]$ and yaw rate $\omega_z \in [-0.5, 0.5]$. Given a commanded velocity, v^d , the reference trajectory is either retrieved from the precomputed gait library by selecting the closest matching forward velocity in the case of HZD, or generated online using the analytic form of the H-LIP gait library, which provides closed-form solutions across the velocity space.

The baseline policy is trained with a manually designed reward composed of several heuristic terms. These include tracking of linear x , y and angular yaw velocity, while penalizing vertical velocity, angular velocity about the x and y axes, joint accelerations, joint velocities, joint torques, and abrupt changes in actions. The reward also discourages deviations from an upright base orientation and enforces joint limit compliance. Additional terms encourage behaviors such as staying upright (“stay alive”), avoiding foot slip during contact, maintaining a nominal hip posture and torso height, ensuring adequate foot clearance, and regulating contact scheduling. Furthermore, the policy is penalized for deviations of the arm and torso joints from predefined reference configurations.

TABLE I: Reward weight coefficients used during training for both HZD-CLF and LIP-CLF.

Reward Term	Weight
Torque penalty w_τ	1×10^{-5}
Action-rate penalty $w_{\Delta a}$	1×10^{-3}
Joint limit penalty $w_{q_{\text{limit}}}$	1.0
CLF tracking reward w_v	10.0
CLF decay penalty $w_{\dot{v}}$	2.0
Holonomic position reward w_{hpos}	4.0
Holonomic velocity reward w_{hvel}	2.0

V. RESULTS

We evaluate three policy variants: a baseline trained with hand-tuned rewards, a H-LIP-based CLF shaped policy (LIP-CLF), and an HZD-based CLF-shaped policy (HZD-CLF). All policies are validated in both sim-to-sim transfer using MuJoCo [30] and on hardware (Fig. 6). The experiment video can be found [31]. The policy runs onboard on an additional laptop mounted to the front of the torso during deployment, which also added additional mass (0.616 kg) to the robot.

CLF Decay Condition (Sim): To evaluate whether reference tracking alone is sufficient, or if enforcing the CLF decay condition provides additional benefit, we conduct an ablation study. Fig. 3 compares two policies: one trained with only the tracking reward (r_v), and another with both the tracking and CLF decay rewards (r_v and $r_{\dot{v}}$). Both policies track

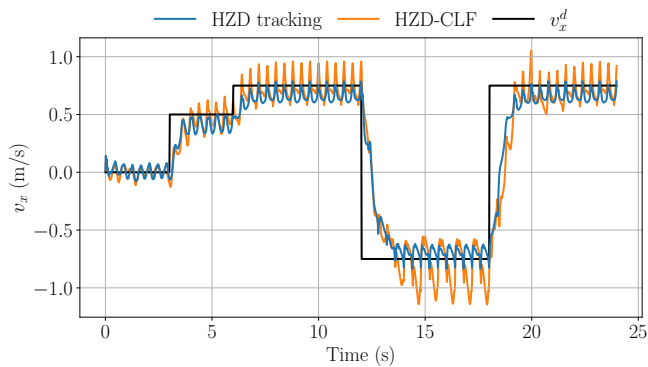


Fig. 3: Tracking performance comparison between a policy trained using only the reference tracking reward (r_v) and one trained with both reference tracking and CLF decrease condition rewards (r_v and $r_{\dot{v}}$). Overall, the HZD-CLF policy achieves better tracking performance

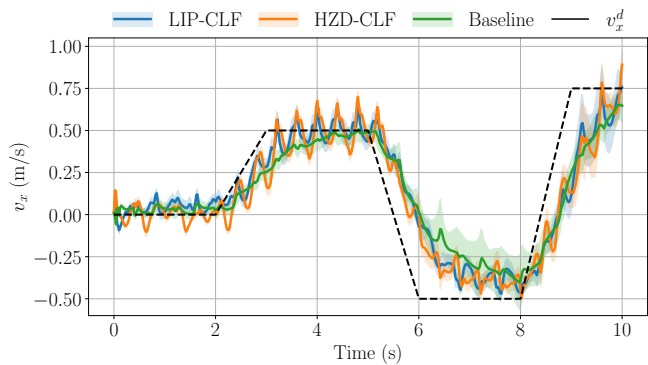


Fig. 4: Tracking performance with torso mass randomly displaced within a box of size $\pm[0.05 (x), 0.05 (y), 0.01 (z)]$ m around the nominal location. Fifty displacements are uniformly sampled, and the resulting mean and standard deviation of performance are plotted. The CLF-RL policies demonstrate lower variability, indicating improved consistency and robustness across different mass configurations.

the commanded velocity v_x^d reasonably well across varying commands. However, the HZD-CLF policy shows improved steady-state tracking, maintaining average velocity closer to the desired value in forward and backward walking phases. While the overall transient behavior remains similar, the inclusion of the CLF decay condition reduces residual tracking error and promotes more consistent steady-state performance.

Mass Location Randomization (Sim): To assess robustness to modeling mismatches, we introduce random perturbations to the torso mass location to simulate sim-to-real discrepancies in inertial properties. Specifically, the torso center of mass is uniformly displaced within a box of size $\pm[0.05 \text{ m } (x), 0.05 \text{ m } (y), 0.01 \text{ m } (z)]$. For each policy, we sample 50 randomized configurations and evaluate the velocity tracking performance across episodes, reporting the mean and standard deviation. As shown in Fig. 4, both CLF-RL policies exhibit significantly lower performance variance

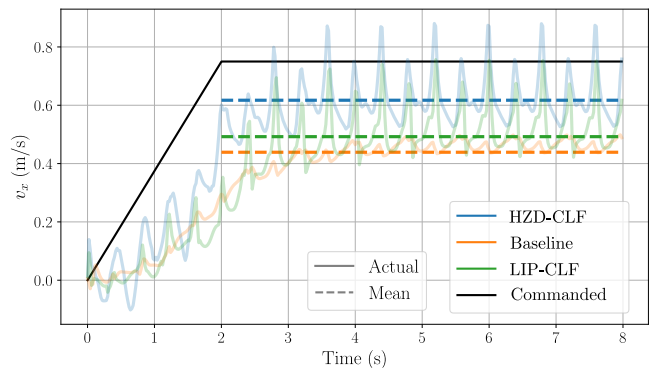


Fig. 5: Robustness testing in simulation with different policies: HZD-CLF, LIP-CLF and a baseline RL policy are compared with an additional 8kg mass added to the torso. A two second ramp up to the maximum trained velocity is commanded. The steady-state mean of the velocities is plotted in a dashed line. The CLF-shaped policies show superior robustness to the baseline.

compared to the baseline. This indicates improved robustness and consistency under structural uncertainties.

Added Mass Perturbation (Sim): To further evaluate robustness, we introduce an 8 kg payload to the torso and compare tracking performance across the three policy variants under a velocity ramp command. As shown in Fig. 5, the CLF-based RL policies maintain more accurate velocity tracking, demonstrating improved resilience to payload-induced dynamics changes.

Indoor Experiments (Hardware): We deploy all policies on the Unitree G1 robot in a controlled indoor environment. Fig. 6 shows all three policies operating successfully on hardware. To quantify velocity tracking performance and robustness, we use a motion capture system to record global position and orientation data. This data is used solely for evaluation and is not fed into the controller. To remain consistent with simulation analysis, we track the pelvis frame and compute local-frame velocity by finite-differencing the position data (recorded at 240 Hz) and aligning it with the robot’s yaw orientation. Fig. 7 demonstrates the improved robustness of the HZD-CLF policy relative to the baseline. To test this robustness, we attach a backpack to the robot and load it with either 1.765 kg or 3.55 kg of additional mass. The HZD-CLF policy maintains consistent tracking performance across all conditions, whereas the baseline policy exhibits significant degradation. In the heavier case, the baseline policy drifts off the walking course and fails to complete the test. These hardware results corroborate the simulation findings in Fig. 4, which show that CLF-based policies exhibit lower performance variance under structural perturbations.

Outdoor Experiments (Hardware): To evaluate the HZD-CLF policy under real-world conditions, we deploy the robot outdoors across a variety of environments. As shown in Fig. 8, the test route includes diverse flat-ground surfaces such as concrete and tiled walkways, as well as mild

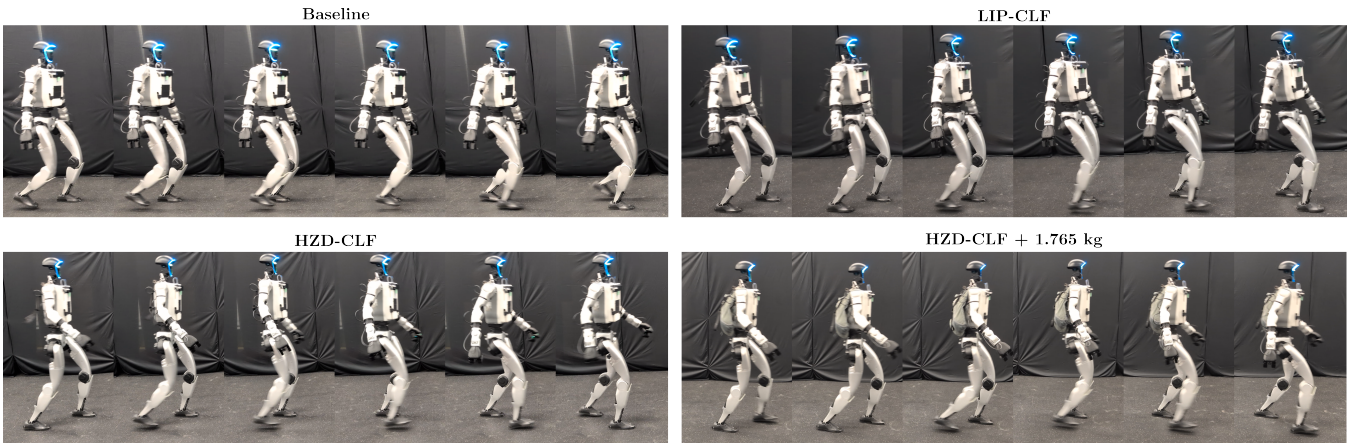


Fig. 6: Snapshots of the three policies throughout a stride on the Unitree G1 robot. These images depict the walking motion in steady state walking with a commanded velocity of $v_x^d = 0.75$ m/s.

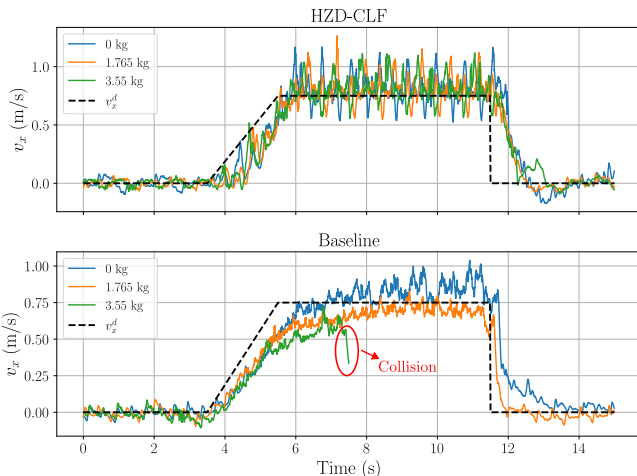


Fig. 7: Quantitative hardware testing shows the difference in robustness of the baseline and HZD-CLF policies. Additional mass is added to a backpack on the back and the velocity tracking is compared. We can see that the HZD-CLF policy has effectively no change in performance with the additional mass. For the heavier mass on the baseline, the policy drifted so much as to exit the walking course and collide with a table, as indicated in the plot.

slopes like ADA-compliant ramps. The robot traverses all terrain types within a single continuous 0.25-mile walking trial without any failures. The distance was determined by experimental design considerations, rather than reflecting any limitation of the policy.

VI. CONCLUSION

We presented CLF-RL, a structured reward shaping framework that integrates reference trajectory tracking with control Lyapunov functions (CLFs). By embedding CLF-based objectives directly into the reinforcement learning reward, our approach replaces heuristic reward design with a theoretically grounded stability metric. We showed that incorporating the CLF decay condition improves tracking performance over

baseline tracking-only rewards. CLF-based policies exhibit lower variance across a range of perturbations in both simulation and hardware, demonstrating increased reliability.

Our framework is modular and extensible. We demonstrated its compatibility with both reduced-order (H-LIP) and full-order (HZD) reference generators, though other trajectory planners could be incorporated. While our training only used steady-state reference motions, the learned policies generalize well to transient motions—highlighting the framework’s flexibility. Finally, we validated the real-world robustness of the approach through extended outdoor trials, showing consistent and stable walking performance across varied flat-ground terrains.

REFERENCES

- [1] E. R. Westervelt, J. W. Grizzle, and D. E. Koditschek, “Hybrid zero dynamics of planar biped walkers,” *IEEE transactions on automatic control*, vol. 48, no. 1, pp. 42–56, 2003.
- [2] J. P. Reher, A. Hereid, S. Kolathaya, C. M. Hubicki, and A. D. Ames, “Algorithmic foundations of realizing multi-contact locomotion on the humanoid robot durus,” in *Algorithmic Foundations of Robotics XII: Proceedings of the Twelfth Workshop on the Algorithmic Foundations of Robotics*. Springer, 2020, pp. 400–415.
- [3] S. Kajita, F. Kanehiro, K. Kaneko, K. Fujiwara, K. Harada, K. Yokoi, and H. Hirukawa, “Biped walking pattern generation by using preview control of zero-moment point,” in *2003 IEEE international conference on robotics and automation (Cat. No. 03CH37422)*, vol. 2. IEEE, 2003, pp. 1620–1626.
- [4] S. Kajita, F. Kanehiro, K. Kaneko, K. Yokoi, and H. Hirukawa, “The 3D linear inverted pendulum mode: a simple modeling for a biped walking pattern generation,” in *Proceedings 2001 IEEE/RSJ International Conference on Intelligent Robots and Systems.*, vol. 1. Maui, HI, USA: IEEE, 2001, pp. 239–246. [Online]. Available: <http://ieeexplore.ieee.org/document/973365/>
- [5] J. Lee, J. Hwangbo, L. Wellhausen, V. Koltun, and M. Hutter, “Learning quadrupedal locomotion over challenging terrain,” *Science robotics*, vol. 5, no. 47, p. eabc5986, 2020.
- [6] Z. Xie, P. Clary, J. Dao, P. Morais, J. Hurst, and M. Panne, “Learning locomotion skills for cassie: Iterative design and sim-to-real,” in *Conference on Robot Learning*. PMLR, 2020, pp. 317–329.
- [7] N. Rudin, D. Hoeller, P. Reist, and M. Hutter, “Learning to Walk in Minutes Using Massively Parallel Deep Reinforcement Learning,” Aug. 2022, arXiv:2109.11978 [cs]. [Online]. Available: <http://arxiv.org/abs/2109.11978>
- [8] Z. Zhuang, S. Yao, and H. Zhao, “Humanoid Parkour Learning,” Sep. 2024, arXiv:2406.10759 [cs]. [Online]. Available: <http://arxiv.org/abs/2406.10759>

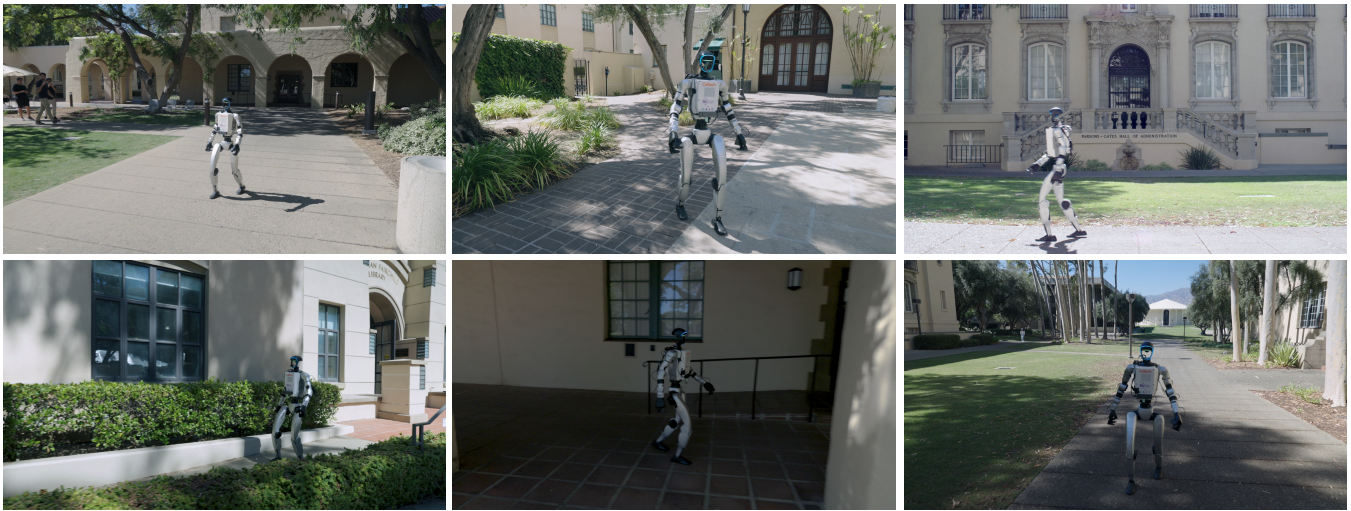


Fig. 8: Demonstration of extensive outdoor testing of the HZD-CLF policy shows its ability to handle diverse flat-ground surfaces, including various tile and concrete types, as well as mild uphill and downhill slopes.

- [9] Z. Li, X. B. Peng, P. Abbeel, S. Levine, G. Berseth, and K. Sreenath, "Reinforcement Learning for Versatile, Dynamic, and Robust Bipedal Locomotion Control," Jan. 2024, arXiv:2401.16889 [cs, eess]. [Online]. Available: <http://arxiv.org/abs/2401.16889>
- [10] R. Batke, F. Yu, J. Dao, J. Hurst, R. L. Hatton, A. Fern, and K. Green, "Optimizing Bipedal Maneuvers of Single Rigid-Body Models for Reinforcement Learning," Jul. 2022, arXiv:2207.04163 [cs]. [Online]. Available: <http://arxiv.org/abs/2207.04163>
- [11] K. Green, Y. Godse, J. Dao, R. L. Hatton, A. Fern, and J. Hurst, "Learning Spring Mass Locomotion: Guiding Policies with a Reduced-Order Model," Mar. 2021, arXiv:2010.11234 [cs]. [Online]. Available: <http://arxiv.org/abs/2010.11234>
- [12] Z. Li, X. Cheng, X. B. Peng, P. Abbeel, S. Levine, G. Berseth, and K. Sreenath, "Reinforcement Learning for Robust Parameterized Locomotion Control of Bipedal Robots," in *2021 IEEE International Conference on Robotics and Automation (ICRA)*. Xi'an, China: IEEE, May 2021, pp. 2811–2817. [Online]. Available: <https://ieeexplore.ieee.org/document/9560769/>
- [13] H. J. Lee, S. Hong, and S. Kim, "Integrating Model-Based Footstep Planning with Model-Free Reinforcement Learning for Dynamic Legged Locomotion," in *2024 IEEE/RSJ International Conference on Intelligent Robots and Systems (IROS)*. Abu Dhabi, United Arab Emirates: IEEE, Oct. 2024, pp. 11 248–11 255. [Online]. Available: <https://ieeexplore.ieee.org/document/10801468/>
- [14] E. D. Sontag, "A Lyapunov-Like Characterization of Asymptotic Controllability," *SIAM Journal on Control and Optimization*, vol. 21, no. 3, pp. 462–471, May 1983. [Online]. Available: <http://epubs.siam.org/doi/10.1137/0321028>
- [15] E. Sontag, "A 'universal' construction of Artstein's theorem on nonlinear stabilization."
- [16] Z. Artstein, "Stabilization with relaxed controls," *Nonlinear Analysis: Theory, Methods & Applications*, vol. 7, no. 11, pp. 1163–1173, Jan. 1983. [Online]. Available: <https://linkinghub.elsevier.com/retrieve/pii/0362546X83900494>
- [17] A. D. Ames, K. Galloway, K. Sreenath, and J. W. Grizzle, "Rapidly Exponentially Stabilizing Control Lyapunov Functions and Hybrid Zero Dynamics," *IEEE Transactions on Automatic Control*, vol. 59, no. 4, pp. 876–891, Apr. 2014. [Online]. Available: <http://ieeexplore.ieee.org/document/6709752/>
- [18] T. Westenbroek, A. Agrawal, F. Castañeda, S. S. Sastry, and K. Sreenath, "Combining Model-Based Design and Model-Free Policy Optimization to Learn Safe, Stabilizing Controllers," *IFAC-PapersOnLine*, vol. 54, no. 5, pp. 19–24, 2021. [Online]. Available: <https://linkinghub.elsevier.com/retrieve/pii/S240589632101243X>
- [19] J. Choi, F. Castañeda, C. J. Tomlin, and K. Sreenath, "Reinforcement Learning for Safety-Critical Control under Model Uncertainty, using Control Lyapunov Functions and Control Barrier Functions," Jun. 2020, arXiv:2004.07584 [eess]. [Online]. Available: <http://arxiv.org/abs/2004.07584>
- [20] T. Westenbroek, F. Castaneda, A. Agrawal, S. Sastry, and K. Sreenath, "Lyapunov Design for Robust and Efficient Robotic Reinforcement Learning," Nov. 2022, arXiv:2208.06721 [cs]. [Online]. Available: <http://arxiv.org/abs/2208.06721>
- [21] S. H. Jeon, S. Heim, C. Khazoom, and S. Kim, "Benchmarking potential based rewards for learning humanoid locomotion," *arXiv preprint arXiv:2307.10142*, 2023.
- [22] B. Morris and J. W. Grizzle, "A restricted poincaré map for determining exponentially stable periodic orbits in systems with impulse effects: Application to bipedal robots," in *Proceedings of the 44th IEEE Conference on Decision and Control*. IEEE, 2005, pp. 4199–4206.
- [23] S. Kajita, F. Kanehiro, K. Kaneko, K. Fujiwara, K. Yokoi, and H. Hirukawa, "A realtime pattern generator for biped walking," in *Proceedings 2002 IEEE International Conference on Robotics and Automation (Cat. No. 02CH37292)*, vol. 1. IEEE, 2002, pp. 31–37.
- [24] X. Xiong and A. Ames, "3-d underactuated bipedal walking via h-lip based gait synthesis and stepping stabilization," *IEEE Transactions on Robotics*, vol. 38, no. 4, pp. 2405–2425, 2022.
- [25] J. Schulman, F. Wolski, P. Dhariwal, A. Radford, and O. Klimov, "Proximal policy optimization algorithms," *arXiv preprint arXiv:1707.06347*, 2017.
- [26] A. Wächter and L. T. Biegler, "On the implementation of an interior-point filter line-search algorithm for large-scale nonlinear programming," *Mathematical Programming*, vol. 106, no. 1, pp. 25–57, Mar. 2006. [Online]. Available: <http://link.springer.com/10.1007/s10107-004-0559-y>
- [27] J. Andersson, J. Gillis, G. Horn, J. Rawlings, and M. Diehl, "CasADi - A software framework for nonlinear optimization and optimal control," *Mathematical Programming Computation*, vol. 11, pp. 1–36, 2019.
- [28] M. Mittal, C. Yu, Q. Yu, J. Liu, N. Rudin, D. Hoeller, J. L. Yuan, R. Singh, Y. Guo, H. Mazhar, A. Mandlekar, B. Babich, G. State, M. Hutter, and A. Garg, "Orbit: A unified simulation framework for interactive robot learning environments," *IEEE Robotics and Automation Letters*, vol. 8, no. 6, pp. 3740–3747, 2023.
- [29] N. Rudin, D. Hoeller, P. Reist, and M. Hutter, "Learning to walk in minutes using massively parallel deep reinforcement learning," in *Proceedings of the 5th Conference on Robot Learning*, ser. Proceedings of Machine Learning Research, vol. 164. PMLR, 2022, pp. 91–100. [Online]. Available: <https://proceedings.mlr.press/v164/rudin22a.html>
- [30] E. Todorov, T. Erez, and Y. Tassa, "Mujoco: A physics engine for model-based control," in *2012 IEEE/RSJ international conference on intelligent robots and systems*. IEEE, 2012, pp. 5026–5033.
- [31] "Supplementary video," <https://youtu.be/f8iuwgCZs3A>.